# A New Construction Method for the Dual Tree Complex Wavelet Based on Direction Sensitivity1)

WANG Hong-Xia CHEN Bo CHENG Li-Zhi

(*Department of Mathematics & System Science, National University of Defense Technology, Changsha* 410073)

(E-mail: whx8292@hotmail.com)

**Abstract** The conception of "main direction" of multi-dimensional wavelet is established in this paper, and the capabilities of several classical complex wavelets for representing directional singularities are investigated based on their main directions. It is proved to be impossible to represent directional singularities optimally by a multi-resolution analysis (MRA) of $L^2(\mathbb{R}^2)$. Based on the above results, a new algorithm to construct Q-shift dual tree complex wavelet is proposed. By optimizing the main direction of parameterized wavelet filters, the difficulty in choosing stop-band frequency is overcome and the performances of the designed wavelet are improved too. Furthermore, results of image enhancement by various multi-scale methods are given, which show that the new designed Q-shift complex wavelet do offer significant improvement over the conventionally used wavelets. Direction sensitivity is an important index to the performance of 2D wavelets.

**Key words** Complex wavelet, main direction, Daubechies complex wavelet, dual tree complex wavelet, image enhancement

## 1 Introduction

In the field of signal processing, the sparse representation for unstable signal is a very important and difficult problem. Recently, many new theories have been proposed to get sparser representations for singular multi-dimension signals, such as ridgelet[1], curvelet[2], contourlet[3] and complex wavelet[4∼8]. In these various methods, ridgelet and curvelet are introduced from constructing directional multidimensional basis, and contourlet comes from designing nonseparable multidimensional filters. But all of their computation costs are too expensive for most applications. At the same time, J. M. Lina presented complex Daubechies wavelet[4], whose wavelet function is complex valued. Another noted representative of complex wavelet—the dual tree complex wavelet (*i.e.*, DTCW), was first introduced by N. Kingsbury for the purpose of getting shift invariant wavelet transforms[5,6]. Due to the special relationship between real and imaginary parts, multidimensional complex wavelet transform is directionally oriented and can be realized efficiently in a separable manner. As a new type of wavelet obtaining preferable balance between direction sensitivity and computational cost, complex wavelet has gathered the interest of many researchers in the latest years[5∼8].

Except the mostly used tensor real admissible wavelet, there are at least three types of complex admissible wavelets: complex Daubechies wavelet[4], Gabor wavelet[9] and DTCW[5]. In this paper, we firstly give the definition of main direction, and then analyze these complex wavelets′ direction sensitivities in detail. It is found that the main direction can efficiently indicate the wavelets′ capability of representing directional signals; DTCW is the most direction sensitive and of the lowest computational complexity in the considered complex wavelets. In the second part of this paper, we further show how to construct a Q-shift DTCW on the principle of optimal main directions, which can overcome the difficulty in [7] — the stopband frequency in the goal function is hard to select. In the last part of this paper, various wavelets including the new designed DTCW are used for image enhancement. The results of experiments show that by designing complex wavelet from main directions, we do get complex wavelet representing directionally signals more efficiently and with better processing performances.

## 2 Main direction of two dimensional wavelets

**Definition 1.** Let $\psi(x,y)$ be the two-dimensional admissible wavelet. The main direction of $\psi(x,y)$ is defined as the direction of line

$$\omega_x^* x + \omega_y^* y = 0 \tag{1}$$

1) Supported by National Natural Science Foundation of P. R. China (10171109), the Special Research Fund for Doctoral Program of Higher Education of P. R. China (20049998006)

Received January 4, 2005; in revised form October 9, 2005

where $(\omega_x^*, \omega_y^*) = \arg\max_{\omega_x,\omega_y} |\hat{\psi}(\omega_x, \omega_y)|$. If we denote

$$\alpha_\psi = \begin{cases} \arctan(-\omega_x^*/\omega_y^*), & \omega_y^* \neq 0 \\ \pi/2, & \omega_y^* = 0 \end{cases}$$

then $\alpha_\psi$ is called the obliquity or the direction of $\psi(x,y)$, where $-\pi/2 < \alpha_\psi \leqslant \pi/2$.

Considering the separability is very important to efficiently realize the multidimensional transform, we now study the property of two-dimensional tensor complex wavelets. Let $\psi(t)$ be one-dimensional admissible wavelet, whose corresponding scaling function exists and is denoted as $\varphi(t)$. The two-dimensional wavelets generated by them are

$$\psi^1(x,y) = \varphi(x)\psi(y),\ \psi^2(x,y) = \psi(x)\varphi(y),\ \psi^3(x,y) = \psi(x)\psi(y) \tag{2}$$

According to Definition 1 we have the following lemma:

**Lemma 1.** 1) Suppose $\psi(t)$ can generate an orthogonal MRA of $L^2(\mathbb{R})$; then the main direction of $\psi^1(x,y)$ is 0.

2) Suppose $\psi(t)$ can generate a biorthogonal MRA of $L^2(\mathbb{R})$; then the main direction of $\psi^1(x,y)$ is 0 or $\pm\alpha$, where $\alpha \neq 0$.

3) If $|\hat{\psi}(\omega)| = |\hat{\psi}(-\omega)|$, where $\hat{\psi}(\omega)$ is the Fourier transform of $\psi(t)$, then the main direction of $\psi^3(x,y)$ defined in formula (2) is $\pm\pi/4$.

**Remark.** If the direction of a wavelet function is $\pm\alpha$, $\alpha \neq 0$, then the singularities with directions of $\alpha$ and $-\alpha$ are aliased in the same subband after wavelet transform. It is disadvantageous to distinguish them from a subband. On the other hand, the biorthogonal wavelet filter banks used in image processing are usually of linear phases, which is impossible to have preferable direction sensitivity.

Furthermore, we have the following theorem by Lemma 1.

**Theorem 1.** 1) All the two-dimensional wavelets generated by tight supported orthogonal or biorthogonal symmetrical real wavelets according to formula (2) only have three directions: $\pi/2$ or $\pm\alpha$, 0 or $\pm(\pi/2-\alpha)$ and $\pm\pi/4$.

2) Two-dimensional complex Daubechies wavelets have three directions altogether: $\pi/2$, 0 and $\pm\pi/4$.

**Proof.** For any real valued function $\psi(t)$ and $\varphi(t)$, we have $|\hat{\varphi}(\omega)| = |\hat{\varphi}(-\omega)|$ and $|\hat{\psi}(\omega)| = |\hat{\psi}(-\omega)|$. By Lemma 1 1)~3), Theorem 1) is true.

Since complex Daubechies wavelet can generate orthogonal MRA of $L^2(\mathbb{R})$[4], and its scaling function $\varphi(t)$ and wavelet function $\psi(t)$ are symmetric and antisymmetric, respectively[12], it means $|\hat{\psi}(\omega)| - |\hat{\psi}(-\omega)|$. Then 2) holds too. □

According to Theorem 1, the wavelets of symmetric $|\hat{\varphi}(\omega)|$ and $|\hat{\psi}(\omega)|$ only have very weak capability for representing directional singularities (all the real wavelets are included in this class). Although complex Daubechies wavelets are complex valued, their capability for representing directional singularities of multidimensional signals is still weak. Furthermore, from Theorem 1 we deduce that the frequency response of ideal complex wavelet should be single sided — the positive or negative part is completely suppressed. This happens to accord with the conclusion by N. Kingsbury[7] in the study of shift-invariant transforms. In the next section we will consider the direction of DTCW.

## 3 The main direction of DTCW

The decomposition structure of one-dimensional DTCW transform (*i.e.*, DTCWT) is depicted in Fig. 1, where $\{H_0^{\mathrm{T}}(z), H_1^{\mathrm{T}}(z)\}$ and $\{G_0^{\mathrm{T}}(z), G_1^{\mathrm{T}}(z)\}$, $T = A, B$ are two pairs of real wavelet analysis filters which correspond to real and imaginary parts of complex wavelet filters respectively. The synthesis part of Fig. 1 is constructed by linking every reconstruction real wavelet filter in the reverse way. If $\varphi^{\mathrm{T}}(t)$ and $\psi^{\mathrm{T}}(t)$, $T = A, B$ are the scaling and wavelet functions corresponding to tree $T$, then the complex scaling function $\varphi(t)$ and wavelet function $\psi(t)$ should be written as

$$\begin{cases} \varphi(t) = \varphi^A(t) + i\varphi^B(t) \\ \psi(t) = \psi^A(t) + i\psi^B(t) \end{cases}, \quad i = \sqrt{-1} \tag{3}$$

By the separability of two-dimensional Fourier transforms for $\psi^k(x,y), k = 1,2,3$, we have the following theorem.

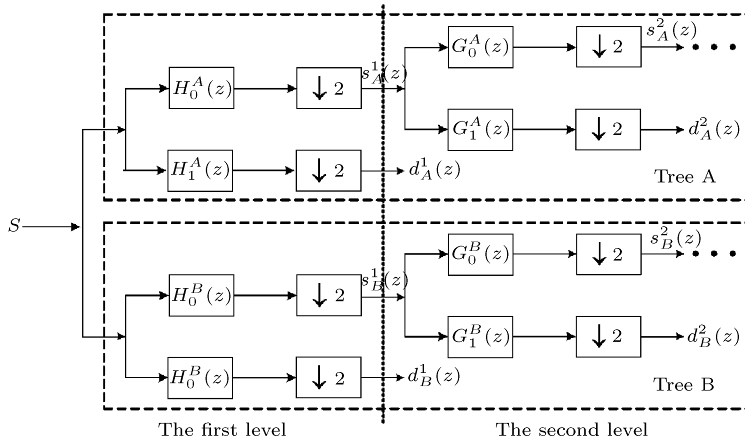


Fig. 1 The decomposition part of 1D DTCWT

**Theorem 2.** 1) Let $\psi^k(x,y), k=1,2,3$ be defined by (2). If the main direction of $\psi^1(x,y)$ is $\alpha$ then $\alpha_{\psi^2} = \underline{\pi/2-\alpha}$, where $\underline{\theta} = \theta \bmod \pi$, $-\pi/2 < \underline{\theta} \leqslant \pi/2$.

2) Define

$$\psi^4(x,y) = \varphi(x)\psi^*(y),\ \psi^5(x,y) = \psi(x)\varphi^*(y),\ \psi^6(x,y) = \psi(x)\psi^*(y) \tag{4}$$

where $*$ represents complex conjugation; then $\alpha_{\psi^4} = -\alpha$, $\alpha_{\psi^5} = \underline{\alpha - \pi/2}$; $\alpha_{\psi^3} = \pi/4$, $\alpha_{\psi^6} = -\pi/4$.

The conclusions in Theorem 2 mean the directions of six complex wavelet functions $\psi^k(x,y), k = 1,2,\cdots,6$ are determined only by $\alpha$-the direction of $\psi^1(x,y)$. If the six directions have a uniform distribution in the two-dimensional plane, the complex wavelet is considered to have strong ability for representing directional singularities. The ideal distribution of six directions for complex wavelets is shown in Fig. 2, where $\alpha = \pi/12$. Fig. 2 is quite similar to the directional partitioning for frequency region of inseparable direction filter banks, which was firstly introduced by R.H. Bamberger in [10]. Note the wavelet transform corresponding to Fig. 2 is separable. Its computational cost is far lower than that in [10].

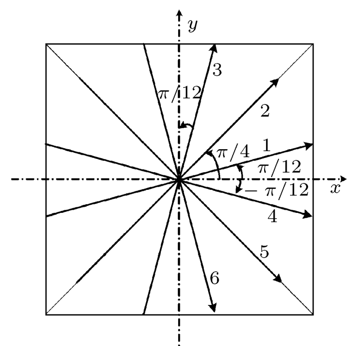


Fig. 2 The ideal distribution of the 2D complex wavelets′ directions

## 4 Design of two-dimensional DTCW based on direction

In the dual tree structure of complex wavelet transform shown in Fig. 1, Q-shift complex wavelet is the most commonly used. The wavelet filters in the first level are both biorthogonal and of odd length. The coefficients of $\{G_0^B(z), G_1^B(z)\}$ in the second level are just the reverse of $\{G_0^A(z), G_1^A(z)\}$. As a result, the construction of Q-shift DTCW is to construct $\{G_0^A(z), G_1^A(z)\}$.

### 4.1 Algorithms for designing DTCW

Note that $G_0^{\mathrm{T}}(z)$, $T = A, B$ are both of even length and $G_0^B(z) = zG_0^A(z^{-1})$ in the Q-shift structure. The complex wavelet system is mainly determined by $G_0^A(z)$ since the wavelet filters in the first level can be chosen as any real biorthogonal wavelet filter of odd length. Here we let $G_1^{\mathrm{T}}(z) = z^{-1}G_0^{\mathrm{T}}(-z^{-1})$. From the perfect reconstruction condition of two band orthogonal filter banks $\{G_0^A(z), G_1^A(z); G_0^A(z^{-1}), G_1^A(z^{-1})$, we have

$$G_0^A(z)G_0^A(z^{-1}) + G_0^A(-z)G_0^A(-z^{-1}) = 1 \tag{5}$$

Denote the coefficients of $G_0^A(z)$ as $\{g(k)\}$, $k = 1-n, \cdots, n$. Then (5) is equivalent to a series of equations about $\{g(k)\}$. The number of equations in (5) together with those from $K$ order regularity and normalized condition is $n+K$ altogether. If $n>K$, there will be some parameters in the solution of the equations. That is to say, $\{g(k)\}$ is parameterized by the parameter set denoted by $\lambda$. Then, different from minimizing the energy of stopband in [7], we choose the optimal parameters by measuring its corresponding main direction. If the direction of $\psi^1(x,y)$ is the closest to $\alpha=\pi/12$, the parameters are just what we need.

So, the process of our design method can be described as follows:

**Algorithm 1.** Construct Q-shift DTCW according to direction sensitivity

1) Let the length of $G_0^A(z)$ be $2n$. Its regular order is $K$. Then denote $P(z)=G_0^A(z)G_0^A(z^{-1})$.

2) Derive $K$ linear equations about $\{g(k)\}$ from regularity, that is $\dfrac{\mathrm{d}^m}{\mathrm{d}z^m}G_0^A(z)\Big|_{z=-1}=0$, $m=0,1,\cdots,K-1$.

3) Get another group of equations about $\{g(k)\}$ from perfect reconstruction condition $P(z)+P(-z)=1$.

4) Put the equations from 2) and 3) and $G_0^A(1)=1$ together to construct an equation set. Then find its solutions $\{g(k)\}$ which is parameterized by $\lambda$. Notice that the equations are easy to solve by Gröbner method[11] In face, the filters to design are always of short lengths ($n$ always is not larger than 6).

5) Considering now the obtained filter banks are only perfect reconstruction and not sufficiently wavelet filters, we should determine the permission set $M$ of $\lambda$ by Daubechies condition[12]:

$$\max_{\omega}|Q(\omega)Q(2\omega)\cdots Q(2^{k-1}\omega)|^{\frac{1}{k}}<2^{K-\frac{1}{2}},\ \text{where } Q(\omega)=G_0^A(\omega)\Big/\left(\frac{1+e^{-i\omega}}{2}\right)^K$$

In the restriction of $\lambda\in M$, we find the optimal parameter $\lambda$ by solving $\min\limits_{\lambda\in M}(\alpha-\pi/12)$. Then $\{g(k)\}$ or $G_0^A(z)$ are known.

6) Obtain $G_0^B(z)$ and $G_1^B(z)$ according to $G_0^A(z)$. Thus the whole complex system is constructed.

### 4.2 Results of construction

The most famous Q-shift complex wavelet is the 6 tap one introduced in [7]. For the convenience to compare, we take $2n=10$, $g(k)=0$ for $k=-2,3,5,6$ as an example to construct DTCW, and let $K=1$. According to steps 1)$\sim$4) of Algorithm 1, we get the filter coefficients as follows

$$\begin{cases} g(-1)=\dfrac{1}{4}(1-|t|);g(2)=\dfrac{1}{4}(1+\sqrt{2-t^2});g(4)=s \\ g(1)=\dfrac{1}{8}(1+|t|+\sqrt{1+t^2+2|t|-16(-1+\sqrt{2-t^2})s-64s^2}) \\ g(-3)=\dfrac{1}{2}-g(-1)-g(1),g(0)=\dfrac{1}{2}-g(2)-g(4)\end{cases} \tag{6}$$

where parameter set $\lambda=(s,t)$.

Fig. 3 shows the relationship of values of $(s,t)$ and the main direction $\alpha$ of $\psi^1(x,y)$. The closer $\alpha$ is to $\pi/12$, the darker the color in Fig. 3. The direction values corresponding to the darkest region in Fig. 3 are listed in Table 1.

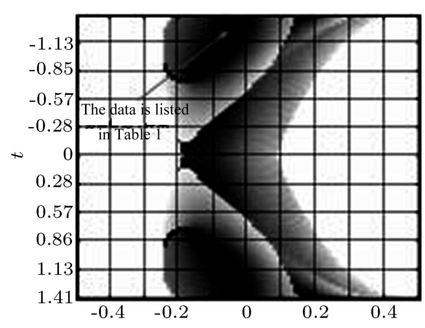


Fig. 3 The direction′s image of $\psi^1(x,y)$ for different values of $s,t$

Table 1 The values for the direction of $\psi^1(x,y)$ for different values of $(s,t)$ (unit: degrees)

| s \ t | −1.386 | −1.357 | −1.329 | −1.301 | −1.273 | −1.244 | −1.216 | −1.188 | −1.159 | −1.131 |
|---|---|---|---|---|---|---|---|---|---|---|
| −0.12 | 10.149 | 11.514 | 13.201 | 15.195 | 16.409 | 17.274 | 17.707 | 17.720 | 17.557 | 33.536 |
| −0.11 | 11.853 | 13.788 | 16.409 | 17.374 | 17.909 | 18.331 | 18.435 | 18.236 | 35.272 | 38.565 |
| −0.10 | 13.456 | 16.731 | 18.012 | 18.225 | 18.747 | 18.538 | 18.536 | 18.239 | 39.333 | 42.230 |
| −0.09 | 16.409 | 18.012 | 18.540 | 18.853 | 18.747 | 18.846 | 18.736 | 38.853 | 23.764 | 22.999 |
| −0.08 | 18.012 | 18.646 | 18.853 | 18.853 | 18.951 | 18.741 | 18.635 | 24.209 | 23.405 | 22.649 |
| −0.07 | 18.329 | 18.646 | 18.853 | 18.853 | 18.951 | 18.741 | 24.864 | 23.839 | 23.044 | 22.297 |
| −0.06 | 18.329 | 18.646 | 18.961 | 18.853 | 18.642 | 25.769 | 24.479 | 23.629 | 22.681 | 21.588 |
| −0.05 | 18.329 | 18.646 | 18.646 | 18.540 | 42.990 | 25.367 | 24.267 | 23.253 | 22.098 | 21.010 |
| −0.04 | 18.116 | 18.329 | 18.329 | 42.955 | 27.440 | 25.346 | 23.654 | 22.652 | 21.354 | 20.283 |
| −0.03 | 17.796 | 18.116 | 42.917 | 39.629 | 27.457 | 24.711 | 23.604 | 22.036 | 20.746 | 19.309 |

The magnitude responses of scaling filters of various designed 6 tap 10/10 Q-shift DTCW are shown in Fig. 4, in which complex wavelets designed by three methods are listed: DTCW_D designed by Algorithm 1 proposed in this paper, DTCW_O designed by N. Kingsbury in [7], DTCW_P by choosing the parameters $(s,t)$ of (6) to optimize the object function in [7]. In Fig. 4 (b), $G(z) = G_0^A(z^2) + z^{-1}G_0^A(z^{-2})$ is to measure the shift-invariant property of the complex wavelet corresponding to $G_0^A(z)$. Fig. 4 indicates that the stopband energy of DTCW_P is a little lower than that of DTCW_O, while that of DTCW_D is the notably lowest in the three. At the same time, the shift-invariant property of DTCW_D is the best comparing with DTCW_P and DTCW_O. That is to say, the performances (such as frequency responses, shift invariance and directional representation ability) of our new designed complex wavelet are more desirable than those proposed before. To construct complex wavelet by optimizing its direction is a reasonable and efficient way.

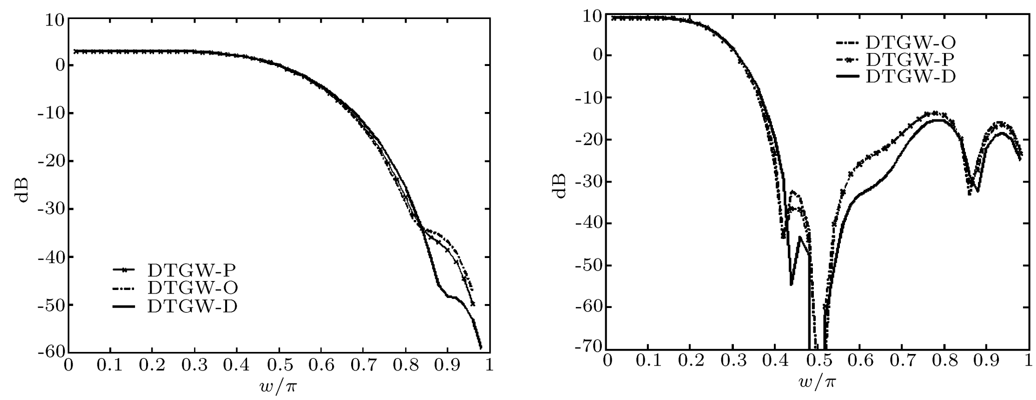


(a) $G_0^A(z)$ (b) $G(z)$

Fig. 4 Magnitude responses of scaling filters of various designed 6 tap 10/10 Q-shift DTCW

Additionally, we can see from the images of DTCW_D listed in Fig. 5 that the complex wavelets designed in this paper are compactly supported and well directional. In fact, a class of complex wavelets of similar performances can be obtained by choosing parameters near their optimal values. Especially, we may get some DTCW filter of all rational coefficients near the optimal one by selecting proper parameters. It is very useful to improve the efficiency of complex wavelet transform since only shift and addition are needed in the transform of rational filters.

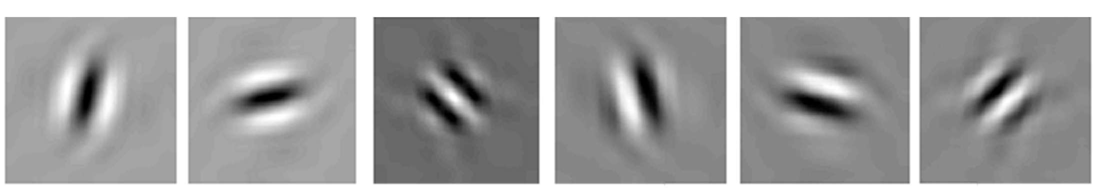

(a) Real part of $\psi^k(x,y)$, $k = 1, 2, \cdots, 6$

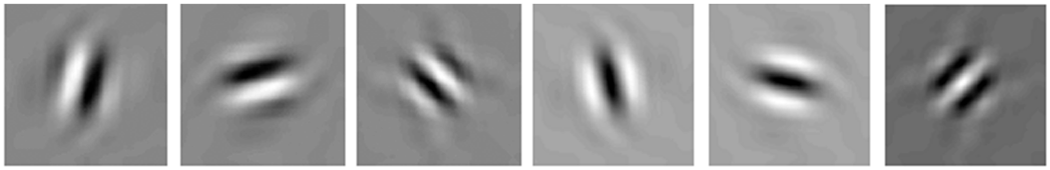

(b) Imaginary part of $\psi^k(x,y)$, $k=1,2,\cdots,6$

Fig. 5 Gray images of the designed 2D DTCW

From the results of constructing complex wavelet filter bank of various lengths, we find that the principle of direction sensitivity is very efficient to get wavelet filters of good properties, such as low stopband energy, ideal shift invariance, without increasing the length of filters or bring additional computations. Compared to the method in [7], the new proposed one in this paper can avoid the troublesome problem to select parameter of stop frequency. Besides, many wavelet filters are obtained together, which makes it easy to select the most suitable one according to special applications.

### 4.3 Image enhancement by DTCW

Since complex wavelet can represent the directional singularities of images better than the classical real wavelet, it is especially appropriate for applications concerning the edges of images such as image denoising, enhancement, edge detection and image partition. In this section, we take image enhancement as an example to illustrate the remarkable influence of wavelets′ directional sensitivity to the processed images. In practice, most of the images to enhance include noise. Noise and the delicate edges of image both correspond to high frequency sub-band after wavelet transform. The most difficult and important thing in enhancement is to distinguish them from the other. Only if the delicate edges are enhanced while noise is suppressed, the visual quality of enhanced image can be desirable.

Noticing that an important difference between noise and edge is the directionality, the edges of images are directional, while noise is not. It is very natural to use DTCWT instead of the widely used real wavelet transform to design the proper enhancing algorithms to get better performances.

Figs. 6 (b)$\sim$(d) are the enhanced images of Fig. 6 (a) by three multiscale enhancing methods — dyadic wavelet transform (DyDWT)[12], Laplacian pyramid decomposition[13] and DTCWT. The bishrink denoising[14] is used in each enhancement process since the original image (a) is visibly noised. What we should remark here is that the denoising processing in DTCWT operates on complex wavelet coefficients directly[15]. Fig. 6 shows that DyDWT can suppress noise quite well, while its enhancing effect is not satisfactory. The index of definition, DEF[16] in Laplacian pyramid decomposition is increased remarkably after enhancing, but the noise is also amplified at the same time, so the visual quality of enhanced image is not satisfactory either. On the other hand, image (d) enhanced by DTCWT behaves the best both in noising suppressing and edge amplifying compared with (c) and (d). DEF of (d) is the maximum in tree enhanced images. And its edges are the most clear. Fingerprint in (d) is easier to identify than that in (a). This result is very helpful for many post-processing such as fingerprint classification and identifying.

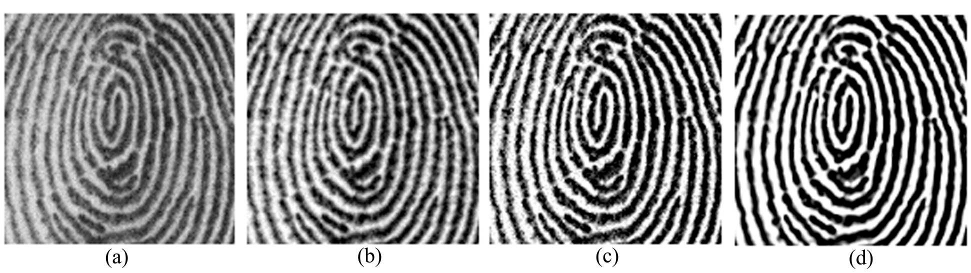


Fig. 6 The enhanced images of standard fingerprint: (a) The original image to be enhanced (DEF=17.86), (b) The enhanced image by DyDWT (DEF=28.60), (c) The enhanced image by Laplace pyramid decomposition (DEF=54.64), (d) The enhanced image by DyDWT (DEF=85.73)

## 5 Concluding remarks

To signify the abilities of wavelet transform for representing directional singularities in multidimensional signal, the term "main direction" is defined in the range of admissible wavelet, and the directional properties of several commonly used multi-dimensional complex wavelets are studied systematically in this paper. We proved that it is impossible to get wavelet of better directional properties than classical real wavelet in a single orthogonal or biorthogonal MRA of $L^2(\mathbb{R})$ without adding parameters or changing the tensor-production format. In all the existing complex wavelets (including the real one as a special example), DTCWT has good performances both in direction property of wavelet and computational efficiency in transform. Considering these facts, a new method for designing Q-shift DTCW filters is introduced and some DTCW with better performances are designed. The image enhanced by DTCWT using the newly designed complex wavelet is more satisfying than those by classical ones. This experiment result approves that main direction is a reasonable and important index of multidimensional wavelet.

In summary, the directional DTCWT gives us an optimal vision for processing multi-dimensional signals especially to the directional singularities. But there are still many problems to study in the future. For example, what is the effect of multi-value main directions to the performances of complex wavelet? Besides, in experiments we find that DTCWT specially suits to process signals with circle characters, but why? We wish to publish our successive results about these problems in the following days.

## References


1 Donoho D L. Orthonormal ridgelets and linear singularities. *SIAM Journal on Mathematical Analysis*, 2000, **31**(5): 1062~1099

2 Starck J L, Candès E J, Donoho D L. The curvelet transform for image denoising. *IEEE Transactions on Image Processing*, 2002, **11**(6): 670~684

3 Do M N, Vetterli M. Contourlets: A directional multiresolution image representation. In: Proceedings of the 2002 International Conference on Image Processing, Rochester, New York, USA: IEEE Press, 2002. **1**: 357~360

4 Lina J M, Mayrand M. Complex Daubechies wavelets. *Applied and Computational Harmonic Analysis*, 1995, **2**: 219~229

5 Kingsbury N. Image processing with complex wavelets. In: Proceedings of Philosophical Transactions of the Royal Society, London: Royal Society A, 1999. **357**(1760): 2543~2560

6 Kingsbury N. A dual-tree complex wavelet transform with improved orthogonality and symmetry properties. In: Proceedings of the 2000 International Conference on Image Processing, Vancouver, Vancouver, BC, Canada: IEEE Computer Society, 2000. **2**: 375~378

7 Kingsbury N. Complex wavelets for shift invariant analysis and filtering of signals. *Applied and Computational Harmonic Analysis*, 2001, **10**: 234~253

8 Tivaz P. Complex wavelet based image analysis and synthesis [Ph. D. dissertation]. Cambridge: Department of Engineering, University of Cambridge, 2000

9 Lee T S. Image representation using 2D Gabor wavelets. *IEEE Transactions on Pattern Analysis and Machine Intelligence*, 1996, **18**(10): 959~971

10 Bamberger R H, Smith M J. A filter bank for the directional decomposition of images: Theory and design. *IEEE Transactions on Signal Processing*, 1992, **40**(7): 882~893

11 Adams W W, Loustaunau P. An Introduction to Gröbner Bases. Graduate Studies in Mathematics, Providence: American Mathematical Society, 1994

12 Mallat S. A Wavelet Tour of Image Processing. London: Academic Press, 1997

13 Dippel S, Stahl M, Wiemker R, et al. Multiscale contrast enhancement for radiographies: Laplacian pyramid versus fast wavelet transform. *IEEE Transactions on Medical Imaging*, 2002, **21**(4): 343~353

14 Sendur L, Selesnick I W. Bivariate shrinkage functions for wavelet-based denoising exploiting interscale dependency. *IEEE Transactions on Signal Processing*, 2002, **50**(11): 2744~2756

15 Wang Hong-Xia, Cheng Li-Zhi, Wu Yi. A complex wavelet based spatially adaptive algorithm for noised image enhancement. *Journal of Computer Aided Design & Computer Graphics*, 2005, **17**(9): 1911~1916

16 Zhang Yu-Jin. Image Partition. Beijing: Science Precess, 2001



**WANG Hong-Xia** Lecturer in the Department of Mathematics & System Science at National University of Defense Technology. Received her Ph. D. degree from National University of Defense Technology in 2004. Her research interests include wavelet analysis, fast numerical algorithms, and image processing.

**CHEN Bo** Ph. D. candidate, received his master degree from National University of Defense Technology in 2004. His research interests include wavelet analysis and image compression.

**CHENG Li-Zhi** Professor in the Department of Mathematics & System Science at National University of Defense Technology. His research interests include wavelet analysis, parallel algorithms, and information theory.